J Physiol 589.8 (2011) pp 2079–2091

The Journal of Physiology

Brain circuits mediating baroreflex bradycardia inhibition in rats: an anatomical and functional link between the cuneiform nucleus and the periaqueductal grey

Florence Netzer[1], Jean-François Bernard[2], Anthony J. M. Verberne[3], Michel Hamon[2], Françoise Camus[1], Jean-Jacques Benoliel[1] and Caroline Sévoz-Couche[1]

[1] *UPMC/INSERM, UMR-S 975 and CNRS UMR 7225, Faculté de médecine UPMC, Site Pitie-Salpêtrière, Paris F-75013, France*
[2] *CPN, INSERM UMR U894, Faculté de médecine UPMC, Site Pitie-Salpêtrière, Paris F-75013, France*
[3] *Department of Medicine, Clinical Pharmacology and Therapeutics Unit, Austin Health, University of Melbourne, Heidelberg, Victoria, 3084, Australia*

Non-technical summary Defence reactions are physiological responses to imminent danger. They include increased blood pressure and heart rate, and a reduction in the reflex cardiac response to changes in blood pressure. Two regions in the brain, the hypothalamus and the periaqueductal grey area, known to be involved in pathological conditions such as anxiety, are involved in the production of these responses. However, there is no direct connection between those regions. In this study we report that the midbrain cuneiform nucleus links the hypothalamus and periaqueductal grey area. Our findings may explain how anxiety is related to cardiovascular pathologies.

Abstract Defence responses triggered experimentally in rats by stimulation of the dorsomedial nucleus of the hypothalamus (DMH) and the dorsolateral periaqueductal grey matter (PAG) inhibit the cardiac baroreflex response (i.e. bradycardia). It has also been proposed that the midbrain cuneiform nucleus (CnF) is involved in active responses. Our aim was to identify the neurocircuitry involved in defence-induced baroreflex inhibition, with a particular focus on the link between DMH, CnF and dorsolateral PAG. Microinjection of the anterograde tracer *Phaseolus vulgaris* leucoaggutinin into the CnF revealed a dense projection to the dorsolateral PAG. Moreover, activation of neurons in the CnF induced increased expression of Fos protein in the dorsolateral PAG. Inhibition of neurons of the CnF or dorsolateral PAG prevented the inhibition of baroreflex bradycardia induced by DMH or CnF stimulation, respectively. These results provide a detailed description of the brain circuitry underlying acute baroreflex modulation by neurons of the DMH. Our data have shown for the first time that the CnF plays a key role in defence reaction-associated cardiovascular changes; its stimulation, from the DMH, activates the dorsolateral PAG, which, in turn, inhibits baroreflex bradycardia.

(Received 8 December 2010; accepted after revision 14 February 2011; first published online 21 February 2011)
Corresponding author C. Sévoz-Couche: UPMC/INSERM, UMR-S 975 and CNRS UMR 7225, Faculté de médecine UPMC, Site Pitie-Salpêtrière, 91 bd de l'Hôpital, Paris F-75013, France. Email: caroline.sevoz-couche@upmc.fr

Abbreviations BP, blood pressure; CnF, cuneiform nucleus; DMH, dorsomedial nucleus of the hypothalamus; HR, heart rate; MBP, mean blood pressure; PAG, periaqueductal grey matter; PHA-L, *Phaseolus vulgaris* leucoagglutinin; PrCnF, pre-cuneiform nucleus.

DOI: 10.1113/jphysiol.2010.203737

Introduction

The dorsomedial nucleus of the hypothalamus (DMH) and the dorsolateral column of the periaqueductal grey (dorsolateral PAG) are key structures involved in the physiological response to acute stress, i.e. the defence reaction (Carrive *et al.* 1987; Lovick, 1993; Keay & Bandler, 2001; De Menezes *et al.* 2009). Electrical stimulation of the DMH induces an array of physiological responses characteristic of the defence reaction including arousal, increases in respiratory rate, blood pressure, heart rate and regional vascular resistance, associated with inhibition of cardiac baroreflex sensitivity (Sévoz-Couche *et al.* 2003), as well as several other parameters that define the baroreflex sigmoid curve (McDowall *et al.* 2006). Both electrical and chemical activation of the dorsolateral PAG induced similar cardiovascular modifications to those seen with DMH activation (Sevoz-Couche *et al.* 2003; Comet *et al.* 2005). Baroreflex inhibition of hypothalamic origin is probably mediated by the PAG since lesions of this region largely attenuate it (Nosaka *et al.* 1993). DMH stimulation induces Fos expression in the dorsolateral PAG (Silveira *et al.* 1995). However, a direct connection between the DMH and dorsolateral PAG seems unlikely, since fibres from the DMH reach the ventral and lateral PAG but not the dorsolateral PAG (Aarnisalo & Panula, 1995; Thompson *et al.* 1996).

The cuneiform nucleus may also participate in defensive behaviour. Fos immunohistochemical mapping of the neuronal circuits associated with distinct facets of fear, revealed activation of neurons in the pre-cuneiform (PrCnF) and the cuneiform (CnF) nuclei in rodents (Kollack-Walker *et al.* 1999; Takahashi *et al.* 2008). In addition, direct stimulation of these regions in anaesthetized rats induces defence responses (Korte *et al.* 1992; Verberne, 1995; Lam & Verberne, 1997), although the effect on baroreflex bradycardia has not been described. The CnF receives projections from the DMH (Bernard *et al.* 1989) and Fos immunoreactivity was observed in the CnF after stimulation of the DMH (Silveira *et al.* 1995). These data suggest that the CnF may be a relay between the DMH and dorsolateral PAG circuit that mediates baroreflex inhibition. However, no specific link between the CnF and the dorsolateral PAG has been reported to date although one study reported retrograde labelling in the CnF after microinjection of wheat germ agglutinin-horseradish peroxidase into a region extending from the dorsal to the lateral PAG (Beitz, 1989).

The principal goal of this study was to identify the neuronal pathway involved in the baroreflex inhibition that occurs during the defence reaction, with a particular attention to the relationships between DMH, CnF and dorsolateral PAG.

Using microiontophoretic application of the anterograde tracer *Phaseolus vulgaris* leucoagglutinin (PHA-L) to different parts of the CnF, we identified a projection from the rostral CnF to the dorsolateral PAG. Fos expression in the PAG region was examined following rostral CnF stimulation with a particular focus on the dorsolateral PAG. In order to establish a functional link between the DMH, the CnF and the dorsolateral PAG, we investigated the effects of stimulation of the DMH on baroreflex cardiac responses following pharmacological inhibition of neurons in the rostral CnF, and those of CnF activation during blockade of the dorsolateral PAG.

Methods

Ethical approval

Procedures involving animals and their care were all conducted in accordance with institutional guidelines, which are in compliance with national and international law policies (Council directive 87-848, 19 October 1987, Ministère de l'Agriculture et de la Forêt, Service Vétérinaire de la Santé et de la Protection Animale; permission no. 75-855 to C.S.-C., institutional ethical policy: A5326-01). The experiments complied with the Guide for the Care and Use of Laboratory Animals published by the US National Institutes of Health (NIH Publication No. 85-23, revised 1996) and are in compliance with the policies and regulations outlined by *The Journal of Physiology* (Drummond, 2009).

General procedures

All experiments were performed using male Sprague–Dawley rats (330–350 g, $n = 72$) kept under controlled environmental conditions (ambient temperature: $21 \pm 1^{\circ}$C, 60% relative humidity, unrestricted access to food and water, alternate 12 h light–12 h dark cycles) for at least 1 week after receipt from the breeding centre (CER Janvier, Le Genest-St Isle, France).

Animals were anaesthetized with urethane (1.5 g kg^{-1}, I.P.) in all experiments in which recovery was not required. The depth of anaesthesia was assessed regularly by pinching a hind-paw and monitoring the stability of arterial blood pressure and heart rate recordings. Rectal temperature was maintained at 37°C with a thermostatically controlled heating blanket. The femoral vein was catheterized for administration of additional anaesthesia or drugs. Systemic blood pressure (BP) and mean BP (MBP) were monitored via a femoral arterial catheter connected to a pressure transducer and DC amplifier (Gould, Courtaboeuf, France). The electrocardiogram (ECG) was recorded using stainless steel pins placed subcutaneously into fore- and hind-paws. Signals were amplified and filtered (Universal Amplifier,

Gould). Heart rate (HR) was computed from the ECG (R wave pulses) and displayed as mean frequency per minute (bin size = 1 s). Anaesthetized animals were placed in a stereotaxic frame with the head fixed in the flat skull position.

Anterograde tracing of CnF efferents and illustration

Rats used for the anterograde tracing experiments ($n = 10$) were anaesthetized with chloral hydrate (400 mg kg^{-1} I.P., 7%). A glass micropipette with an outside tip diameter of 20–30 μm was filled with a solution of 5% PHA-L (Vector Laboratories, Burlingame, CA, USA). After craniotomy, the micropipette was positioned in the CnF with reference to a standard atlas of the rat brain (Paxinos & Watson, 2005): 2 mm lateral to the midline, 5 mm ventral to the brain surface, and from −8.0 to −8.3 mm (rostral sites) or −8.5 to −8.8 mm (caudal sites) caudal to bregma. Iontophoretic application of PHA-L was made by passing direct current (2–6 μA, electrode tip positive) through the micropipette for 20 s per 30 s period, for 20 min. Following a postoperative survival time of 15 days, animals were deeply anaesthetized with pentobarbital (200 mg kg^{-1}, I.P.). They were then perfused transcardially with phosphate-buffered saline (PBS; 0.12 M, pH 7.4) containing 4% paraformaldehyde, 0.1% glutaraldehyde and 0.05% picric acid, and the brain was removed and cryoprotected in 20% sucrose solution for 5 days. Frozen sections (50 μm thick) of the whole brainstem were collected in four containers filled with PBS, allowing their parallel processing as free-floating sections (Bernard *et al.* 2008). These sections were divided into three series, two being processed for PHA-L immunochemistry (Bourgeais *et al.* 2001).

Briefly, two series of sections were incubated overnight in the primary antibody (goat anti-PHA-L; 1/1000, Vector Laboratories), rinsed in PBS, incubated for 1 h in the secondary antibody (rabbit biotinylated anti-goat; 1.5/200, Vector), rinsed again, and finally incubated in the avidin–biotin–horseradish peroxidase solution (one drop of reagent A plus one drop of reagent B complex per 10 ml, ABC vectastain kit, Vector). The sections were then rinsed in PBS. One series of sections was processed with DAB only (Sigma, St Louis, MO, USA), using progressively increasing concentrations of H_2O_2 (0.001%, 0.003%, 0.007%, 0.015%, 0.040%), and a second series of sections was processed with the DAB–nickel enhanced technique, using similarly increasing H_2O_2 concentrations. The third series of sections, not processed with immunohistochemistry, was counterstained with cresyl violet before being coverslipped.

Each injection site was analysed from a series of camera lucida drawings (150 μm apart) of coronal sections processed with DAB only. Injection sites (containing the stained cells) were identified by superimposition onto adjacent Nissl-stained sections. The labelled fibres were observed under brightfield illumination in coronal sections. Terminals were differentiated from fibres *en passage* using classical morphological criteria (ramifications, varicosities, thickness and pattern). Images were exported to Adobe Photoshop (v. 9/CS2) in order to reconstruct them and to adjust brightness and contrast. Stained fibres were drawn and additional indications and anatomical landmarks were inserted.

Fos expression in PAG following pharmacological activation of the rostral CnF

Two unilateral (left side) microinjections of (–)-bicuculline methiodide (50 pmol/50 nl) (with 10 min interval) were made at rostral sites that project to the dorsolateral PAG (i.e. approximately −8.2 mm from bregma) in order to maintain CnF activation for 20 min, as confirmed by a sustained increase in MBP. This dose of bicuculline corresponded to those employed previously to induce changes in baroreflex curve parameters when injected in the DMH (McDowall *et al.* 2006) or the dorsolateral PAG (Comet *et al.* 2005). Rats either received microinjections into the rostral CnF of saline (Sham group, $n = 10$) or bicuculline methiodide (Experimental group, $n = 12$). Two series of frozen sections were collected to allow parallel processing. Immunolabelling was performed as described previously (Bernard *et al.* 2008). Briefly, sections were incubated overnight in the primary antibody (rabbit anti-Fos; 1/8000, K-25, Santa Cruz Biotechnology Inc., Santa Cruz, CA, USA), rinsed with PBS, incubated for 1 h in the secondary antibody (biotinylated goat anti-rabbit, 1/200, BA1000, Vector Laboratories), rinsed again, and finally incubated in the avidin–biotin–horseradish peroxidase solution (one drop of reagent A plus one drop of reagent B complex per 10 ml, ABC vectastain kit, Vector). The sections were then rinsed in PBS followed by rinsing in Tris buffer (0.12 M, pH 7.4) before reacting with 0.04% 3,3′-diaminobenzidine (DAB, Sigma-Aldrich, St Quentin-Fallavier, France) + 0.2% ammonium nickel sulfate (Sigma-Aldrich) supplemented with H_2O_2 every 4 min in order to obtain H_2O_2 increasing concentrations (0.00015%, 0.0003%, 0.0006%, 0.0012%, 0.0024%, 0.0048%). After an extensive final rinsing, one series was mounted on gelatin-coated slides and coverslipped.

For each animal, a total of four brain sections were analysed under brightfield illumination. Neurons were plotted using Mercator software (Explora Nova, La Rochelle, France). The computer was connected to (1) a CCD colour video camera which captured images and supplied red, green and blue output, and (2) an XY stage microscope stage controller which sent the

micrometric location of the section boundaries to the computer. We counted Fos labelled cells in different columns of the PAG, after careful individual examination of each neuron at high magnification (×40). The outline of the section and the main structures were drawn at low magnification (×4, ×10), the computer providing continuous synchronization between plotting and section location during moving or magnification changes. The criterion for identification of Fos labelled neurons included the presence of dark black or brown reaction product in a round structure corresponding to the cell nucleus.

Baroreflex activation

The baroreceptors were unloaded using the vasodilator agent sodium nitroprusside (100 μg kg^{-1}, I.V.) followed by baroreceptor stimulation using the vasoconstrictor agent phenylephrine (10 μg kg^{-1}, I.V.) when the nitroprusside-induced depressor response had reached the nadir. This treatment produced changes in MBP ranging from −40 to +50 mmHg, respectively, and HR changes ranging from +50 to −180 bpm, respectively. Phenylephrine alone was used when muscimol was microinjected. We observed that the time between two tests of combined sodium nitroprusside/phenylephrine or phenylephrine alone must be of at least 10 min for the reproducibility of the repeated reflex responses.

Evaluation of baroreflex activity

Reflex changes in heart rate in response to phenylephrine-induced changes in MBP were analysed by two means. First, the maximal bradycardic coefficient was calculated as the ratio of the maximal cardiac response after the phenylephrine injection to the HR baseline value, over the maximal increase in MBP (ΔMBP) (in mmHg^{-1} = 100 × (ΔHR/HR baseline)/ΔMBP). Second, administration of nitroprusside followed by phenylephrine allowed the generation of baroreceptor function curves by fitting the data to the sigmoid logistic function:

$$Y = \text{Bottom} + (\text{Top} - \text{Bottom}) /(1 + \exp((V_{50} - X)/\text{Slope}),$$

using GraphPad Prism (GraphPad Software Inc., La Jolla, CA, USA), where Bottom and Top are the lower and higher HR plateau values, Top – Bottom is the baroreflex range, and V_{50} is the value of MBP at the mid-point of the curve. The Maximal gain (i.e. baroreflex sensitivity, related to the maximal slope at V_{50}) was calculated as follows:

$$\text{Maximal gain} = -\text{range} \times (-1/\text{slope})/4.$$

Pharmacological activation of the DMH or CnF

As detailed above, a single-barrel glass micropipette (outer diameter <100 μm) connected to a Hamilton microsyringe filled with a selective $GABA_A$ receptor antagonist ((–)-bicuculline methiodide; 50 pmol/50 nl) was directed toward the left DMH (AP –3.0; LAT 0.5; DV –8.5, in mm from bregma, Paxinos & Watson, 2005) or the rostral CnF (at sites mentioned above, i.e. −8.2 caudal to bregma). Defence reaction activation was identified by the observation of somatic defence responses such as mydriasis, vibrissae and body movements, and tail erection.

Bicuculline was microinjected into the DMH ($n = 5$) and rostral CnF ($n = 5$) in non-pretreated animals, to observe characteristic increases in MBP and HR.

To eliminate the influence of defence reaction-induced tachycardia on the cardiac baroreflex responses, all animals used in the following experiments were pre-treated with the β-adrenoceptor antagonist atenolol (1 mg kg^{-1}, I.V., 20 min before baroreflex induction).

Effects of pharmacological activation of the DMH or CnF on the cardiac baroreflex

Intravenous injections of nitroprusside and phenylephrine were made before ('Control') and during ('Experimental') pharmacological activation of the DMH ($n = 10$) or rostral CnF ($n = 10$), i.e. when the increase in blood pressure due to bicuculline microinjection was at its maximum (i.e. after approximately 2 min).

Effects of pharmacological blockade of the CnF on the baroreflex inhibition induced by DMH activation

Muscimol (500 pmol/100 nl) was microinjected into the rostral CnF using a single-barrel glass micropipette (outer diameter <100 μm) connected to a Hamilton microsyringe. This dose was in the middle range of that employed previously to inhibit cardiovascular modifications induced by the DMH when injected into the dorsolateral PAG (de Menezes *et al.* 2006).

Intravenous administration of phenylephrine was performed before ('Control') and during pharmacological activation of the DMH ('Experimental'). Reflex responses to phenylephrine were elicited before ('Control 1' and 'Experimental 1') and 15 min after ('Control 2' and 'Experimental 2') microinjections of muscimol into the CnF ($n = 5$).

Effects of pharmacological blockade of the dorsolateral PAG on the baroreflex inhibition induced by CnF activation

Three bilateral microinjections of muscimol (500 pmol/100 nl) were made into the dorsolateral

PAG. All were located 0.5 mm lateral to the midline and 4 mm ventral to the brain surface and at several rostrocaudal locations: −6.7, −7.0 and −7.3 mm from bregma. This was done to ensure neuronal inhibition was induced in a large area of the PAG.

Pressor responses to phenylephrine were evoked before ('Control') and during pharmacological activation of the CnF ('Experimental'). Reflex heart rate responses to phenylephrine were elicited before ('Control 1' and 'Experimental 1') and 15 min after ('Control 2' and 'Experimental 2') microinjections of muscimol into the dorsolateral PAG ($n = 5$).

Histological localization of microinjection and stimulation sites

Microinjection sites were visualized by the location of the micropipette track and pontamine sky blue deposit in 70 μm thick sections of brain tissue previously fixed in 10% formalin solution and cryoprotected in 20% sucrose solution for 5 days.

Statistical analyses

Student's paired t test (GraphPad Prism 4) was used to assess (1) the cardiac baroreflex responses recorded before and during ('Control' and 'Experimental', respectively) pharmacological activation of the CnF and the dorsolateral PAG, and (2) the increases in MBP and HR induced either by DMH or CnF pharmacological activation.

Student's unpaired t test (GraphPad Prism 4) was used to compare Fos expression in PAG in Experimental (CnF activation) *versus* Sham (no CnF activation) experiments.

Baroreflex bradycardia before ('Control 1 and Experimental 1') and after ('Control 2 and Experimental 2') muscimol microinjections into the CnF or the dorsolateral PAG, were analysed using a two-way repeated measures ANOVA (SigmaStat 3.1; Systat Software Inc.,

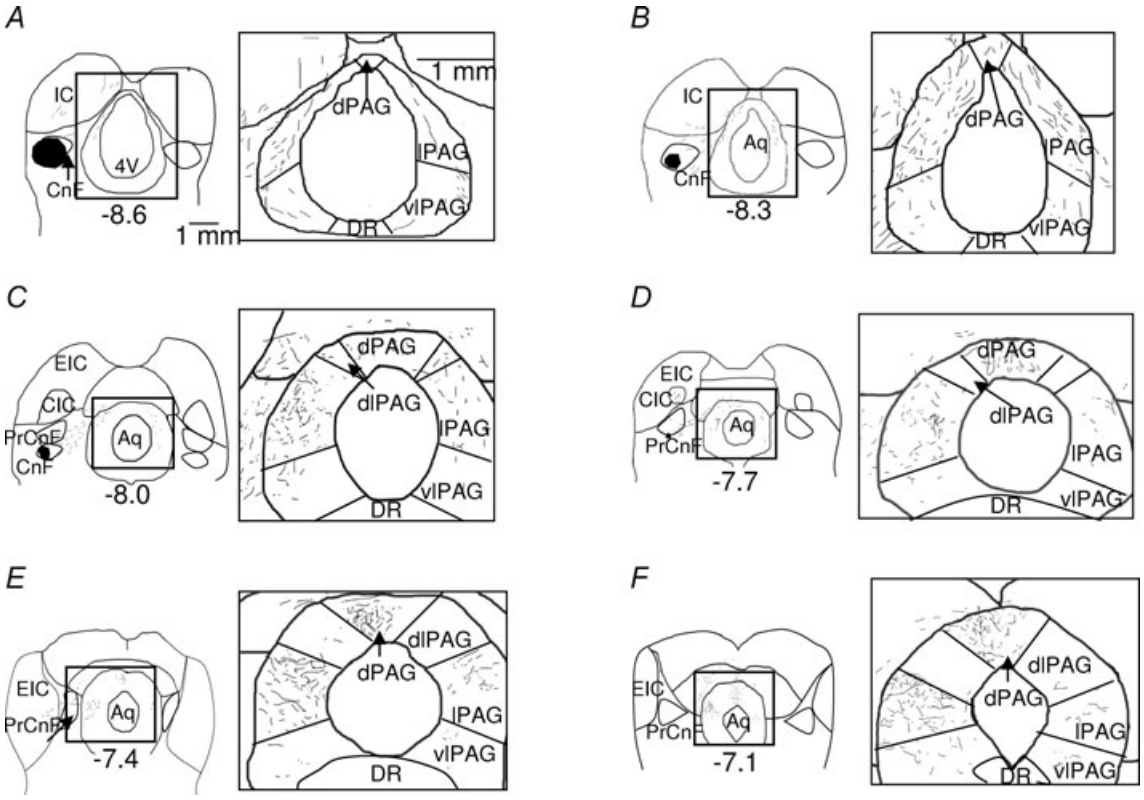

Figure 1. Projections from the caudal CnF to the dorsal and lateral PAG
Camera lucida drawings of anterograde labelling of ascending axons and terminal boutons from an injection of PHA-L in the caudal cuneiform nucleus. Series of transverse sections from posterior to anterior (*A–F*) are shown (×4 and ×10 magnification on the left and right side, respectively). Numbers indicate distance (in mm) from bregma. Abbreviations: 4V: 4th ventricle; Aq: aqueduct; CnF: cuneiform nucleus; dPAG: dorsal column of the periaqueductal grey area; dlPAG: dorsolateral column of the periaqueductal grey area; CIC: central nucleus of the inferior colliculus; DR: dorsal raphé; EIC: external cortex of the inferior colliculus; IC: inferior colliculus; lPAG: lateral column of the periaqueductal grey area; PrCnF: precuneiform nucleus; vlPAG: ventrolateral column of the periaqueductal grey area.

San Jose, CA, USA) (two factor repetition: brain region stimulation and microinjections). Control 1, Control 2, Experimental 1 and Experimental 2 responses were recorded in the same animals. This ANOVA allowed a cross-analysis followed by a *post hoc* Bonferroni/Dunn correction due to interactions (Table 2).

All differences were considered significant at $P < 0.05$.

Results

Anatomical link between the CnF and the dorsolateral PAG

Injection of PHA-L was performed at different rostro-caudal sites covering the entire CnF from rostral (from −8.0 to −8.3 mm from bregma) to caudal (−8.5 to

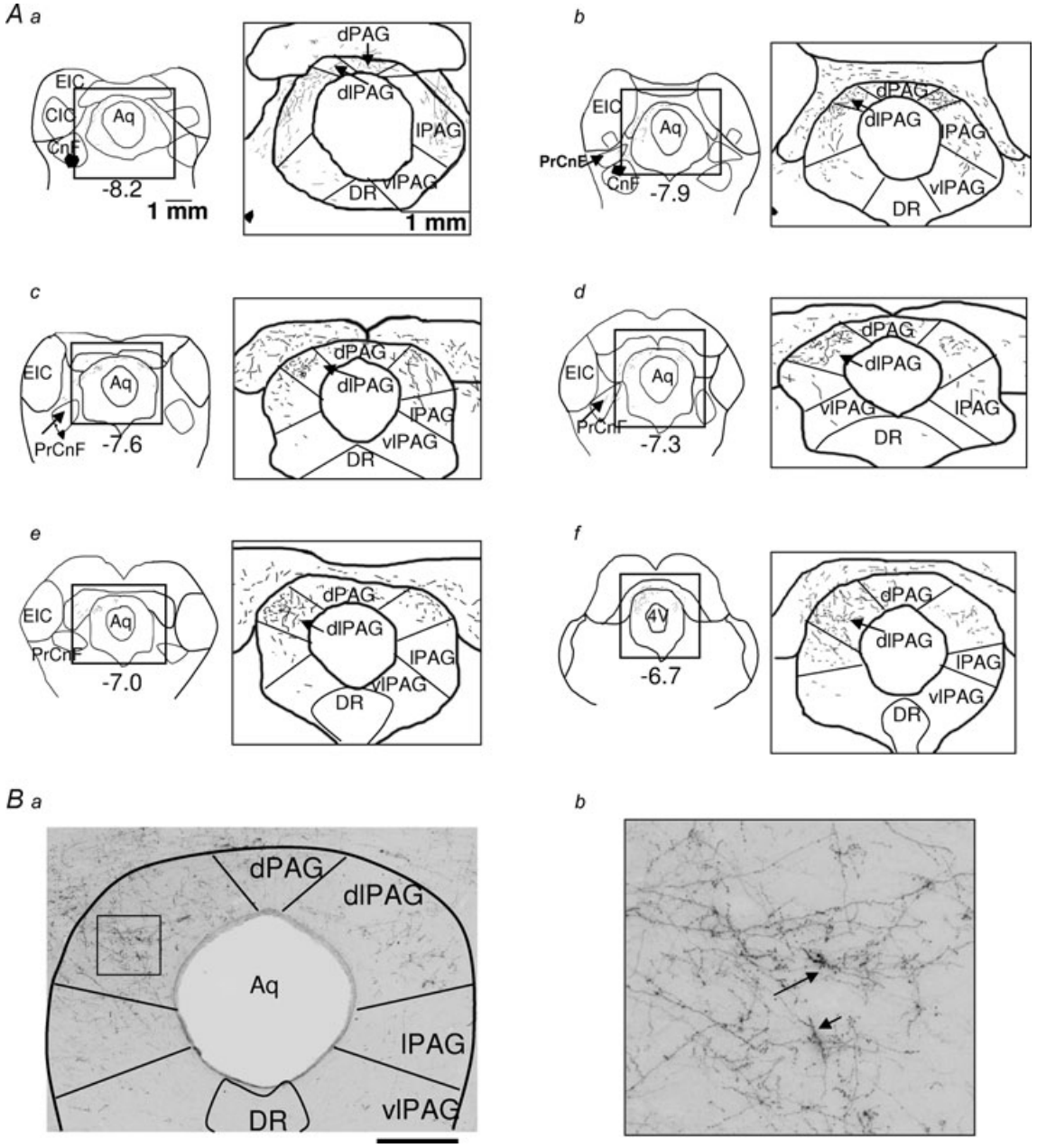

Figure 2. Projections from the rostral CnF to the dorsolateral PAG
A, camera lucida drawings of anterograde labelling of ascending axons and terminal boutons from an injection of PHA-L in the rostral cuneiform nucleus. Series of transverse sections from posterior to anterior (*Aa–f*) are shown (×4 and ×10 magnification on the left and right side, respectively). Numbers indicate distance (in mm) from bregma. *B*, phtotomicrographs corresponding to the drawing shown in *Af*. PHA-L immunolabelled fibres (*Ba*) and varicosities (see arrows in ×20 magnification photomicrograph in *Bb*) in the dorsolateral PAG. Scale bars: 500 μm. For abbreviations, see Fig. 1.

−8.8 mm from bregma). In all cases, the large majority of labelled fibres extending from the CnF to the PAG were found ipsilateral to the site of tracer injection but some were also noted contralaterally.

Fine labelled fibres and ramifications, bearing numerous varicosities, were observed in different columns of the PAG depending on the PHA-L injection site. When PHA-L was injected at caudal locations (Fig. 1), labelled fibres ran through the inferior colliculus and terminated in dorsal and lateral PAG columns; only a few were found in the ventral and dorsolateral regions. In contrast, after injection of PHA-L at more rostral sites (Fig. 2), fibres and boutons appeared to be particularly concentrated in the dorsolateral PAG. The maximum density of labelled fibres was found in an area that produced maximal baroreflex inhibition when stimulated (Comet *et al.* 2005), i.e. at approximately −6.8 to −7.2 mm from bregma. Some fibres were also found in the dorsal region, and very few were observed in the ventral and lateral parts of the PAG.

Fos expression in the PAG after CnF stimulation

Fos expression was analysed in the dorsolateral PAG and immediate surroundings (i.e. dPAG and lPAG) in Sham ($n = 10$) and Experimental ($n = 12$) animals after pharmacological activation of the rostral CnF (Fig. 3*A*). CnF activation evoked a more than 10-fold increase in Fos expression in the ipsilateral PAG and a 3-fold increase in the contralateral dorsolateral PAG of Experimental animals compared to Sham animals ($P < 0.005$ and $P = 0.03$, respectively, Fig. 3*A*). An example of the increase in Fos expression in the dorsolateral PAG is shown in Fig. 3*B*. A small but significant elevation in the number of Fos labelled cells was also found in the ventral PAG (135 ± 10 *vs.* 200 ± 37, respectively, $P = 0.04$).

No difference was found in other parts of the PAG. Indeed, the numbers of Fos neurons in Sham and Experimental animals were 35 ± 10 and 50 ± 8 ($P = 0.6$) in the dorsal PAG, 55 ± 15 and 65 ± 10 in the lateral (both sides) PAG ($P = 0.2$).

Pharmacological activation of the DMH and CnF

In animals that were not pretreated with atenolol, substantial increases in blood pressure (+40 mmHg and +35 mmHg, respectively) and HR (+65 bpm and +72 bpm, respectively), were evoked by activation of neurons in the DMH ($n = 5$, Fig. 4*Aa*) and the rostral CnF (approximately −8.2 mm from bregma, $n = 5$, Fig. 4*Ab*) using microinjections of bicuculline (1 mm).

Effects of pharmacological activation of the DMH or CnF on the cardiac baroreflex response

Tachycardia induced by nitroprusside was not affected by either intra-DMH (Fig. 4*B*) or intra-CnF (Fig. 4*C*)

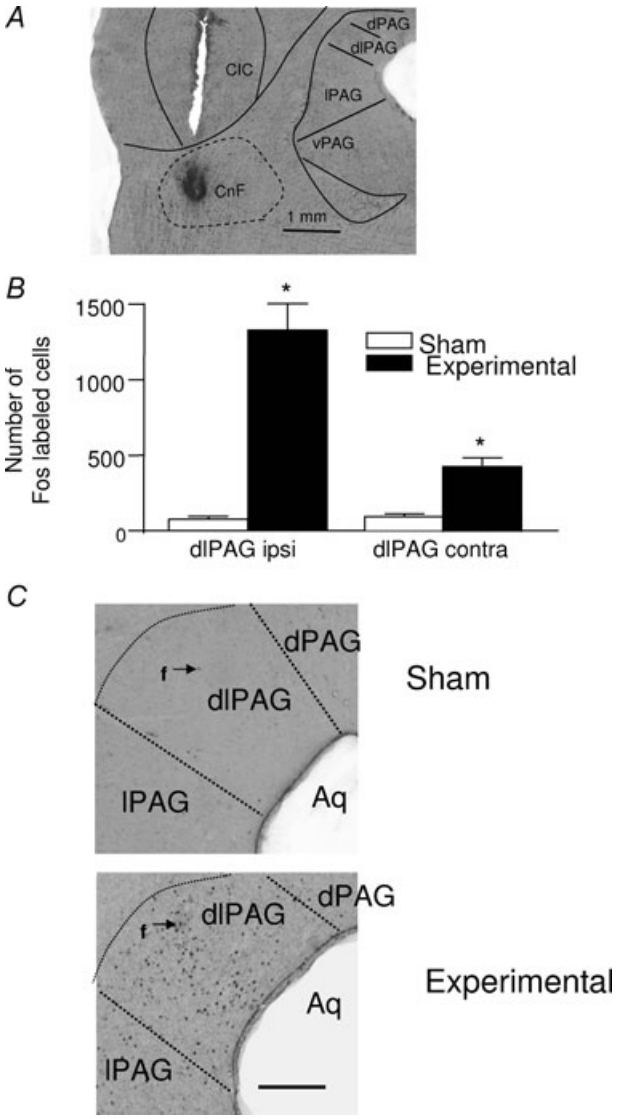

Figure 3. Increase in Fos expression in the dorsolateral PAG after rostral CnF stimulation
A, photomicrographs displaying the CnF site (pontamine sky blue deposit at the very tip of the microelectrode track), at approximately 8.2 mm caudal to bregma, whose activation produced the maximal inhibition of the baroreflex bradycardia. For abbreviations, see Fig. 1. *B*, bar graph showing the number of cells (in four brain sections) expressing Fos protein immunoreactivity in ipsilateral (ipsi) as well as contralateral (contra) dorsolateral PAG (dlPAG), in Sham (open bars, $n = 10$) and Experimental (local application of bicuculline, 50 pmol/0.05 μl; filled bars, $n = 12$) rats. Each bar is the mean ± SEM. *$P < 0.05$. *C*, photomicrographs showing the dense Fos protein immunolabelling (dark core, f) in the dlPAG compared to other parts of the PAG in a rat, after pharmacological activation of the CnF (Experimental) compared to a Sham rat. Scale bar: 500 μm.

injections of bicuculline ($P = 0.65$ and 0.52, respectively). In contrast, the baroreflex bradycardia evoked by phenylephrine (Control) was reduced by 69% during activation of the DMH (Experimental, Fig. 4*B*, $n = 10$, $P < 0.005$) and 75% during activation of the rostral CnF (Experimental, Fig. 4*C*, $n = 10$, $P < 0.0001$). These results were assessed by the diminution of parameters (notably the baroreflex gain) calculated from the baroreflex curves (Fig. 5*A* and *B*, respectively, Table 1). In addition, in support of our findings from anatomical experiments, the percentage inhibition of the baroreflex bradycardia decreased when bicuculline was injected either in anterior (−7.5 mm from bregma) or posterior (−8.6 mm from bregma) sites in the CnF ($n = 15$, Fig. 6).

These experiments indicated that only the phenylephrine-induced bradycardia, but not the tachycardia evoked by nitroprusside injection, was affected by either CnF or DMH stimulation. Therefore, the baroreflex activation produced by phenylephrine was examined in subsequent experiments.

Effects of pharmacological inactivation of the rostral CnF on the inhibition of the baroreflex bradycardia induced by DMH activation

Microinjection of muscimol into the rostral CnF ($n = 5$) did not affect basal MBP (98 ± 7 *vs.* 92 ± 7 mmHg, $P = 0.8$), HR (305 ± 12 *vs.* 309 ± 7 bpm, $P = 0.8$), or increase in MBP induced by pharmacological DMH activation (38 ± 4 mmHg vs. 40 ± 5 mmHg, $P = 0.8$, Fig. 7).

The inhibition of the baroreflex bradycardia induced by DMH activation was −75% and −18%, before and after intra-CnF muscimol, respectively ($P = 0.005$, Fig. 7). Before muscimol treatment (Fig. 7*A*), baroreflex gain was reduced (Bonferroni's multiple comparison test, Table 2) from -5.1 ± 0.4 bpm mmHg^{-1} (Control 1) to -2.6 ± 0.4 bpm mmHg^{-1} (Experimental 1). After microinjection of muscimol into the rostral CnF (Fig. 7*B*), the baroreflex gain was -5.3 ± 0.6 bpm mmHg^{-1} prior to DMH activation (Control 2)) compared to -4.3 ± 0.5 bpm mmHg^{-1} during DMH activation

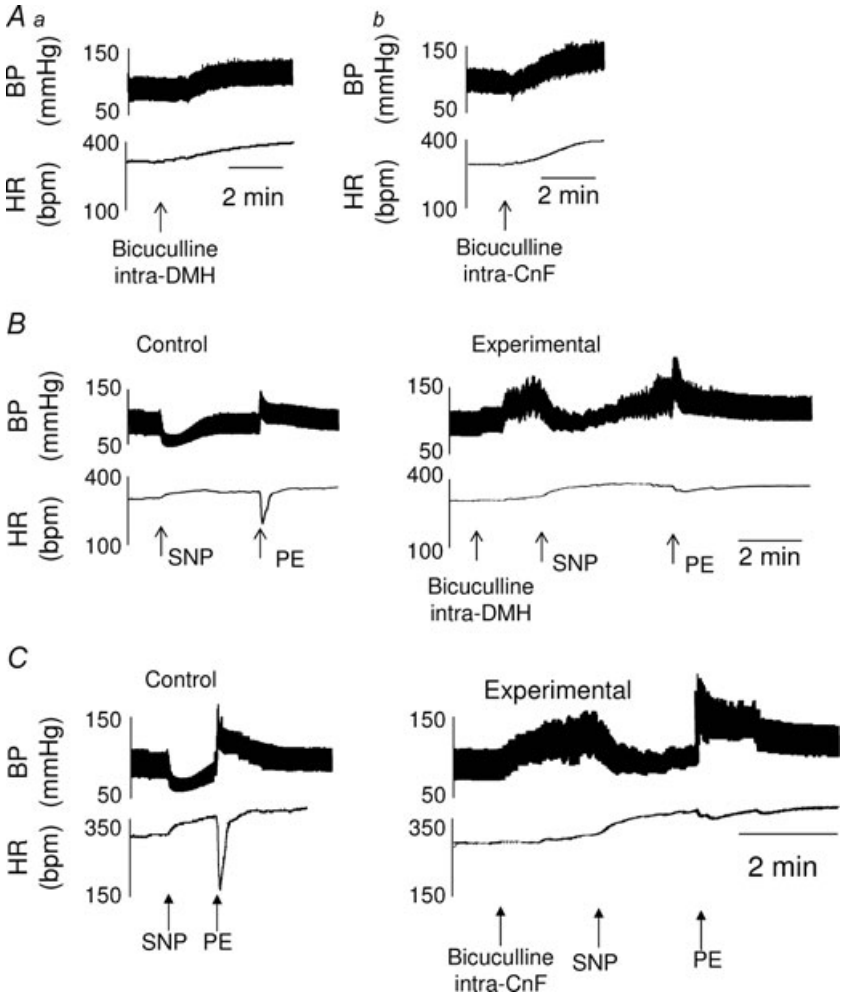

Figure 4. Inhibition of the baroreflex bradycardia after chemical activation of the DMH and the rostral CnF
A, representative recordings illustrating that pharmacological activation of the dorsomedial nucleus of the hypothalamus (DMH, 100 pmol/0.1 μl, *Aa*) or the rostral cuneiform nucleus (rostral CnF, *Ab*), by local application of bicuculline (50 pmol/50 μl), increased the MBP and HR in an animal not pretreated with atenolol. In addition, in atenolol-pretreated rats, DMH (*B*) or CnF (*C*) pharmacological activation did not affect the baroreflex tachycardia induced by administration of the vasodilator nitroprusside but inhibited the reflex bradycardia induced by administration of the vasoconstrictor phenylephrine.

Table 1. Parameters of the baroreflex curves from rats ($n = 23$), before or during pharmacological stimulation of either the DMH or rostral CnF

	Before DMH	During DMH	*P*	Before CnF	After CnF	*P*
Upper HR plateau (bpm)	366 ± 22	370 ± 10	0.9	343 ± 12	360 ± 13	0.6
Lower HR plateau (bpm)	110 ± 15	290 ± 10	< 0.005*	131 ± 10	262 ± 11	< 0.005*
Range (bpm)	256 ± 17	80 ± 10	< 0.001*	212 ± 11	97 ± 10	0.01*
V_{50} (mmHg)	100 ± 8	98 ± 3	0.35	106 ± 5	103 ± 4	0.25
Maximal gain (bpm mmHg^{-1})	−4.9 ± 0.3	−1.1 ± 0.5	< 0.005*	5.6 ± 0.3	1.4 ± 0.1	< 0.005*

Values are mean ± SEM.

(Experimental 2)) (Bonferroni's multiple comparison test, Table 2).

Effects of pharmacological inactivation of the dorsolateral PAG on the inhibition of the baroreflex bradycardia induced by CnF activation

Microinjections of muscimol into the dorsolateral PAG ($n = 5$) did not affect basal MBP (90 ± 2 *vs.* 98 ± 7 mmHg, $P = 0.8$), HR (305 ± 10 *vs.* 309 ± 10 bpm, $P = 0.9$), nor the increase in MBP induced by rostral CnF pharmacological activation (30 ± 1 mmHg and 35 ± 1 mmHg, $P = 0.5$, Fig. 8).

Prior to microinjection of muscimol into the dorsolateral PAG, activation of the rostral CnF inhibited the cardiac baroreflex response to phenylephrine by 78% (Bonferroni's multiple comparison test between Control 1 and Experimental 1 maximal bradycardic coefficients, Fig. 8*A*), and reduced the baroreflex gain by the same percentage (-4.7 ± 0.6 bpm mmHg^{-1} before (Control 1) compared to -1.1 ± 0.4 bpm mmHg^{-1} during (Experimental 1) CnF activation). In the same rats, bilateral microinjection of muscimol into the dorsolateral PAG reduced the inhibition of the baroreflex bradycardia by CnF activation to only –25% (Fig. 8*B*) (Table 2). Accordingly, the maximal gain of the sigmoid curve was of -4.8 ± 0.6 bpm mmHg^{-1} before (Control 2) compared to -4.1 ± 0.3 bpm mmHg^{-1} during (Experimental 2) CnF activation, $P < 0.001$).

Discussion

The most striking result of the present study is that the rostral CnF is a relay in the pathway between the DMH and the dorsolateral PAG that inhibits baroreflex bradycardia.

As reported by Carrive and collaborators (Zhang *et al.* 1990), stimulation of the dorsolateral column of the PAG evoked characteristic autonomic and behavioural responses of the fight/flight (defence) reaction while the ventrolateral column activation produced immobility. We used the anterograde tracer PHA-L applied to rostral and caudal sites in the CnF, and looked specifically for projections to the dorsolateral PAG. We found that only the rostral CnF sends projections almost exclusively to the dorsolateral column of the PAG. It should be emphasized that Fos expression in the dorsolateral PAG was found in a limited area, approximately −7 mm caudal to bregma. This region corresponds exactly to the site where microstimulation exerts the maximal inhibitory influence on baroreflex bradycardia (Comet *et al.* 2005). Labelled fibres from caudal CnF PHA-L injections innervated the dorsal PAG, in support of the work of Lam *et al.* (1996) that showed an increase in Fos messenger RNA

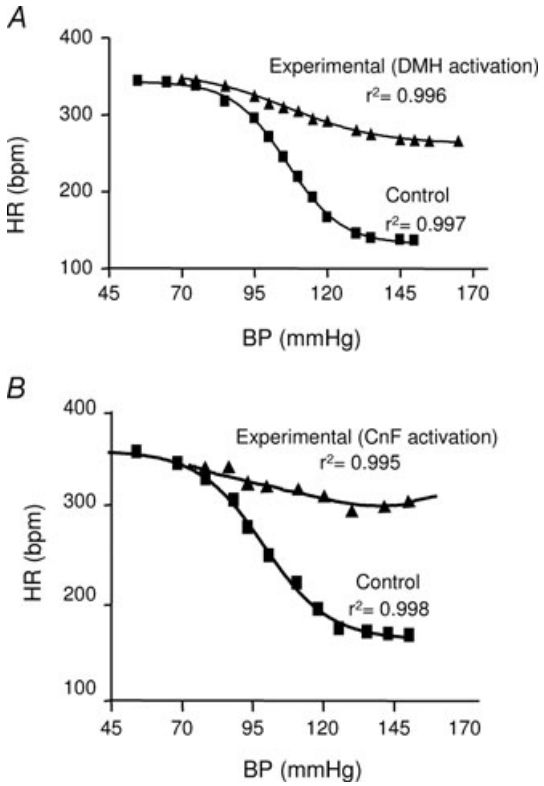

Figure 5. Reduction of the baroreflex curve slopes after DMH and rostral CnF stimulation
Baroreflex curves depicting the change in HR in response to MBP changes corresponding to rats shown in Fig. 4*B* and *C*, before (Control) and during (Experimental) pharmacological stimulation of the DMH (*A*) or rostral CnF (*B*).

levels in the dorsal PAG after caudal CnF stimulation. We also performed PHA-L injection in the PrCnF and observed convergent fibres to the dorsal and lateral but not dorsolateral PAG (data not shown), confirming previous anterograde (Korte *et al.* 1992) and autoradiographic studies (Edwards, 1975; Zemlan & Behbehani, 1988).

Drastic increased expresssion of FOS was observed in the dorsolateral PAG, after activation of the rostral CnF. Activated cells in the dorsolateral PAG were again found at approximately −7 mm caudal to bregma. A small variation of labelled cells in the ventral PAG was also observed, which may be explained by interconnections between dorsolateral and ventral PAG; indeed it was observed previously that Fos expression increased in the ventral PAG after dorsolateral PAG stimulation (Bernard *et al.* 2008).

Activation of both DMH and CnF induced inhibition of baroreflex bradycardia without affecting the reflex cardiac responses to the vasodilator nitroprusside. Sites within the CnF where stimulation produced the maximal inhibitory effect on the baroreflex bradycardia corresponded to the rostral CnF, which also projects to and activates neurons in the dorsolateral PAG. Indeed, baroreflex inhibition was less prominent when injections were made caudally or rostrally to these regions, and did not occur when injection sites were outside the CnF. Neurons in the DMH and rostral CnF were activated using the $GABA_A$ receptor antagonist bicuculline, implying that local neurons and not fibres *en passage* were activated.

In addition to the neuroanatomical observations we examined the effects of the DMH and the rostral CnF activation on the cardiac baroreflex using classical sigmoidal curve fitting. This allowed us to determine HR responses across the full range of BP excursions. Calculation of the maximal gain gives information on the maximal baroreflex sensitivity (Head & McCarty, 1987): this was clearly reduced after activation of the DMH or the rostral CnF. Thus, activation of neurons in the rostral CnF was found to induce not only arousal responses and modifications of resting cardiovascular parameters, but also the inhibition of baroreflex bradycardia. Taken together, this study suggests that the rostral CnF, along with the DMH and dorsolateral PAG, can be considered as a crucial component of neurocircuitry of the defence reaction.

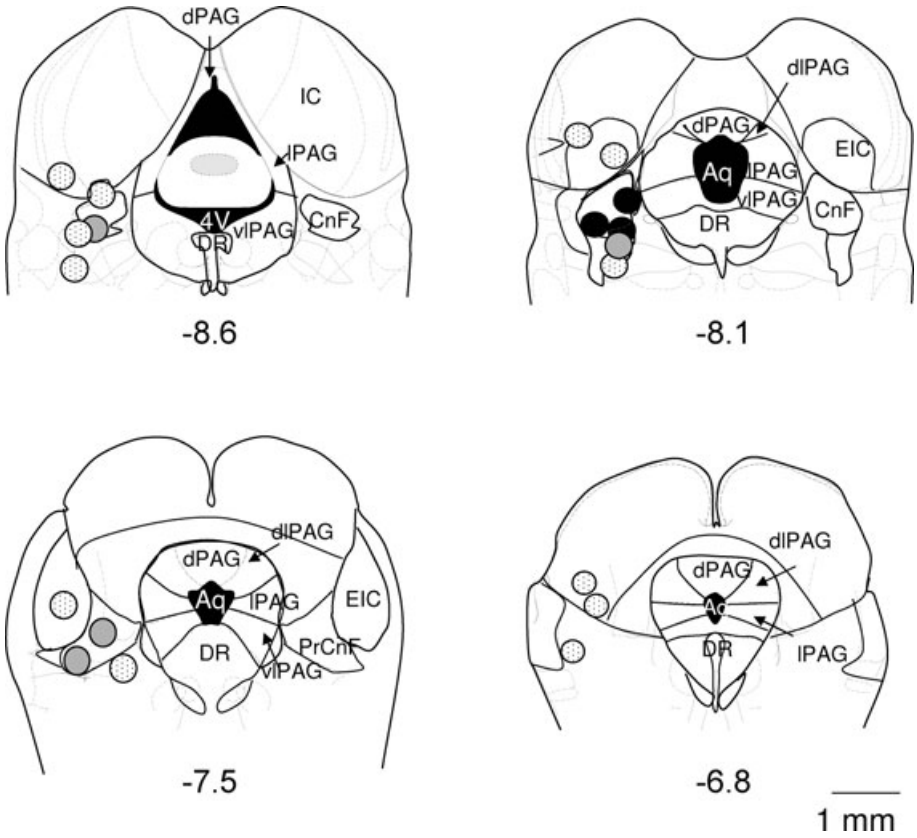

Figure 6. Maximal inhibition of the baroreflex inhibition after activation of the rostral CnF
Coronal sections (modified from Paxinos & Watson, 2005) showing representative sites of bicuculline microinjections in the CnF. The resulting baroreflex bradycardia inhibition was more than 60% (black circles), 20–60% (grey circles) or of less than 20% (dotted circles). Numbers indicate distance (in mm) from bregma. For abbreviations, see Fig. 1.

Microinjection experiments using the inhibitory agent muscimol were performed to establish the connectivity between the DMH, the rostral CnF and the dorsolateral PAG. We found that inhibition of neurons in the rostral CnF prevented the inhibitory effect of DMH activation on baroreflex bradycardia (but not the DMH-induced rise in blood pressure). In addition, microinjection of muscimol into the dorsolateral PAG reduced the rostral CnF stimulation-induced inhibition of the baroreflex. It is possible that muscimol microinjected into the dorsolateral PAG diffused to the CnF, thereby contributing to a reduced inhibitory effect on the baroreflex bradycardia. However, that seems unlikely because body movements and increases in blood pressure characteristic of defensive responses were still observed after CnF stimulation despite muscimol microinjections made into the dorsolateral PAG.

Conversely, blockade of the DMH did not reduce the inhibitory effect induced by electrical CnF stimulation on the baroreflex bradycardia; in the same manner, inactivation of the CnF did not affect the dorsolateral PAG-induced baroreflex inhibition (data not shown).

Table 2. Statistical analysis of the interaction between the effects of CnF or dorsolateral PAG pharmacological stimulation and intra-cerebral microinjections of muscimol, on the baroreflex bradycardia using two-way repeated measures ANOVA

DMH	$F(1/3) = 20.1$, $P = 0.005$*
CnF saline	$F(1/3) = 0.2$, $P = 0.7$
DMH × CnF saline	$F(1/3) = 5.4$, $P = 0.2$
DMH	$F(1/4) = 21.5$, $P = 0.005$*
CnF muscimol	$F(1/4) = 2.0$, $P = 0.1$
DMH × CnF muscimol	$F(1/4) = 13.2$, $P = 0.01$*
CnF	$F(1/3) = 15.2$, $P = 0.03$*
Dorsolateral PAG saline	$F(1/3) = 1.2$, $P = 0.7$
CnF × dorsolateral PAG saline	$F(1/3) = 2.8$, $P = 0.5$
CnF	$F(1/4) = 19.1$, $P = 0.005$*
Dorsolateral PAG muscimol	$F(1/4) = 2.0$, $P = 0.4$
CnF × dorsolateral PAG muscimol	$F(1/4) = 20.2$, $P = 0.001$*

Taken together, these data clearly support the idea that the DMH acts on the rostral CnF that, in turn, activates the dorsolateral PAG, to lead to baroreflex inhibition.

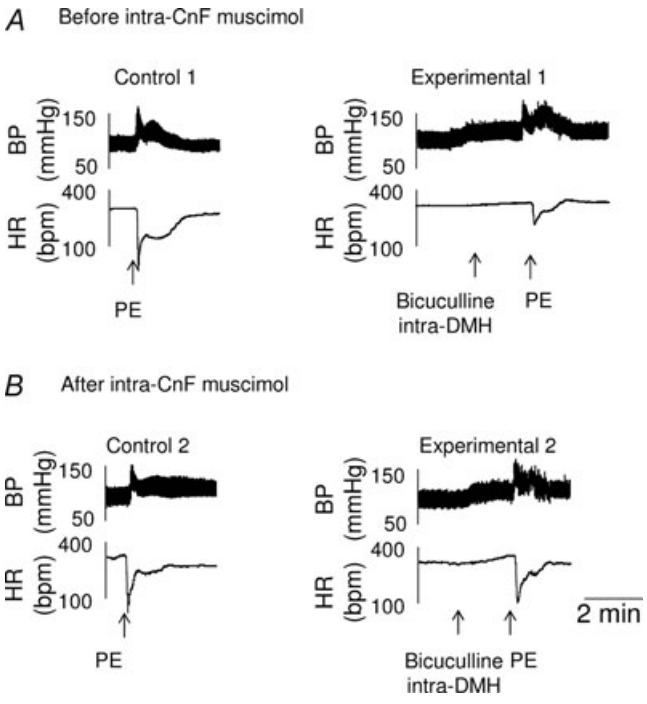

Figure 7. Prevention of the inhibition of baroreflex bradycardia produced by pharmacological activation of the DMH, following microinjection of muscimol into the CnF
A, representative recordings showing that the reflex bradycardic response to phenylephrine administration (Control 1) prior to intra-CnF muscimol ($n = 5$), was markedly reduced by intra-DMH bicuculline (Experimental 1). *B*, after the application of muscimol into the CnF, DMH activation exerted only a minor non-significant effect on the reflex bradycardic response to PE (see Experimental 2 *versus* Control 2). Each group is the mean ± SEM. *$P < 0.005$.

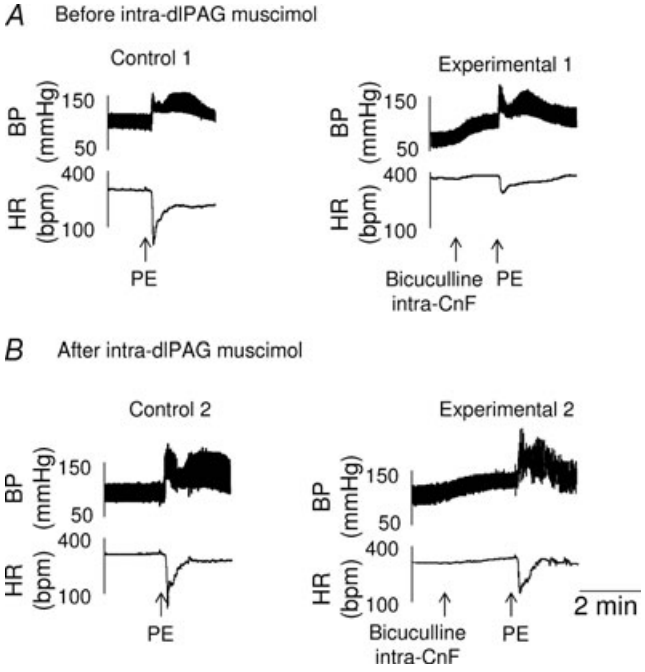

Figure 8. Prevention of the inhibition of baroreflex bradycardia inhibition produced by pharmacological activation of the CnF following microinjection of muscimol into the dorsolateral PAG
Representative recordings showing that the baroreflex cardiac response inhibition normally occurring during CnF activation (compare Control 1 and Experimental 1 in *A*, $n = 5$) was reversed by microinjection of muscimol into the dlPAG (*B*). Each group is the mean ± SEM. *$P < 0.005$.

The study presented here is based on cardiac modification (i.e. baroreflex bradycardia inhibition) in physiological stress like in the defence reaction. However, the structures studied here are also involved in chronic stress such as occurs in panic disorder or anxiety. Disinhibition of the DMH showed also significant increases in plasma levels of both ACTH and corticosterone, indexes of stress axis activation (see in DiMicco *et al.* 2002), and muscimol in DMH increased social interaction in rats (Shekhar, 1994). In addition, the periaqueductal grey is activated by mild anxiogenic stress (Devall & Lovick, 2010) and is suggested as part of the pathway involved in panic disorders (Graeff & Del-Ben, 2008). Finally, the CnF contributes to anxiety and neophobia (Walker & Winn, 2007). Our data provide evidence of a central pathway that can explain the link existing between anxiety and reduction in the baroreflex control of HR (Watkins *et al.* 1998).

References

Aarnisalo AA & Panula P (1995). Neuropeptide FF-containing efferent projections from the medial hypothalamus of rat: a *Phaseolus vulgaris* leucoagglutinin study. *Neuroscience* **65**, 175–192.

Beitz AJ (1989). Possible origin of glutamatergic projections to the midbrain periaqueductal gray and deep layer of the superior colliculus of the rat. *Brain Res Bull* **23**, 25–35.

Bernard JF, Netzer F, Gau R, Hamon M, Laguzzi R & Sevoz-Couche C (2008). Critical role of B3 serotonergic cells in baroreflex inhibition during the defense reaction triggered by dorsal periaqueductal gray stimulation. *J Comp Neurol* **506**, 108–121.

Bernard JF, Peschanski M & Besson JM (1989). Afferents and efferents of the rat cuneiformis nucleus: an anatomical study with reference to pain transmission. *Brain Res* **490**, 181–185.

Bourgeais L, Gauriau C & Bernard JF (2001). Projections from the nociceptive area of the central nucleus of the amygdala to the forebrain: a PHA-L study in the rat. *Eur J Neurosci* **14**, 229–255.

Carrive P, Dampney RL & Bandler R (1987). Excitation of neurones in a restricted portion of the midbrain periaqueductal grey elicits both behavioural and cardiovascular components of the defence reaction in the unanaesthetised decerebrate cat. *Neurosci Lett* **81**, 273–278.

Comet MA, Laguzzi R, Hamon M & Sevoz-Couche C (2005). Functional interaction between nucleus tractus solitarius NK1 and 5-HT3 receptors in the inhibition of baroreflex in rats. *Cardiovasc Res* **65**, 930–939.

De Menezes RC, Zaretsky DV, Fontes MA & DiMicco JA (2006). Microinjection of muscimol into caudal periaqueductal gray lowers body temperature and attenuates increases in temperature and activity evoked from the dorsomedial hypothalamus. *Brain Research* **1092**, 129–137.

De Menezes RC, Zaretsky DV, Fontes MA & DiMicco JA (2009). Cardiovascular and thermal responses evoked from the periaqueductal grey require neuronal activity in the hypothalamus. *J Physiol* **587**, 1201–1215.

Devall AJ & Lovick TA (2010). Differential activation of the periaqueductal gray by mild anxiogenic stress at different stages of the estrous cycle in female rats. *Neuropsychopharmacology* **35**, 1174–1185.

DiMicco JA, Samuels BC, Zaretskaia MV & Zaretsky DV (2002). The dorsomedial hypothalamus and the response to stress: part renaissance, part revolution. *Pharmacol Biochem Behav* **71**, 469–480.

Drummond GB (2009). Reporting ethical matters in *The Journal of Physiology*: standards and advice. *J Physiol* **587**, 713–719.

Edwards SB (1975). Autoradiographic studies of the projections of the midbrain reticular formation: descending projections of nucleus cuneiformis. *J Comp Neurol* **161**, 341–358.

Graeff FG & Del-Ben CM (2008). Neurobiology of panic disorder: from animal models to brain neuroimaging. *Neurosci Biobehav Rev* **32**, 1326–1335.

Head GA & McCarty R (1987). Vagal and sympathetic components of the heart rate range and gain of the baroreceptor-heart rate reflex in conscious rats. *J Auton Nerv Syst* **21**, 203–213.

Keay KA & Bandler R (2001). Parallel circuits mediating distinct emotional coping reactions to different types of stress. *Neurosci Biobehav Rev* **25**, 669–78.

Kollack-Walker S, Don C, Watson SJ & Akil H (1999). Differential expression of Fos mRNA within neurocircuits of male hamsters exposed to acute or chronic defeat. *J Neuroendocrinol* **11**, 547–559.

Korte SM, Jaarsma D, Luiten PG & Bohus B (1992). Mesencephalic cuneiform nucleus and its ascending and descending projections serve stress-related cardiovascular responses in the rat. *J Auton Nerv Syst* **41**, 157–176.

Lam W, Gundlach AL & Verberne AJ (1996). Increased nerve growth factor inducible-A gene and c-fos messenger RNA levels in the rat midbrain and hindbrain associated with the cardiovascular response to electrical stimulation of the mesencephalic cuneiform nucleus. *Neuroscience* **71**, 193–211.

Lam W & Verberne AJ (1997). Cuneiform nucleus stimulation-induced sympathoexcitation: role of adrenoceptors, excitatory amino acid and serotonin receptors in rat spinal cord. *Brain Res* **757**, 191–201.

Lovick TA (1993). The periaqueductal gray-rostral medulla connection in the defence reaction: efferent pathways and descending control mechanisms. *Behav Brain Res* **58**, 19–25.

McDowall LM, Horiuchi J, Killinger S & Dampney RA (2006). Modulation of the baroreceptor reflex by the dorsomedial hypothalamic nucleus and perifornical area. *Am J Physiol Regul Integr Comp Physiol* **290**, R1020–R1026.

Nosaka S, Murata K, Inui K & Murase S (1993). Arterial baroreflex inhibition by midbrain periaqueductal grey in anaesthetized rats. *Pflugers Arch* **424**, 266–275.

Paxinos G & Watson C (2005). *The Rat Brain in Stereotaxic Coordinates*, 5th edn. Academic Press, London.

Sevoz-Couche C, Comet MA, Hamon M & Laguzzi R (2003). Role of nucleus tractus solitarius 5-HT3 receptors in the defense reaction-induced inhibition of the aortic baroreflex in rats. *J Neurophysiol* **90**, 2521–2530.

Shekhar A (1994). Effects of treatment with imipramine and clonazepam on an animal model of panic disorder. *Biol Psychiatry* **36**, 748–758.

Silveira MC, Sandner G, Di Scala G & Graeff FG (1995). C-fos immunoreactivity in the brain following electrical or chemical stimulation of the medial hypothalamus of freely moving rats. *Brain Res* **674**, 265–274.

Takahashi LK, Chan MM & Pilar ML (2008). Predator odor fear conditioning: current perspectives and new directions. *Neurosci Biobehav Rev* **32**, 1218–1227.

Thompson RH, Canteras NS & Swanson LW (1996). Organization of projections from the dorsomedial nucleus of the hypothalamus: a PHA-L study in the rat. *J Comp Neurol* **376**, 143–173.

Verberne AJ (1995). Cuneiform nucleus stimulation produces activation of medullary sympathoexcitatory neurons in rats. *Am J Physiol Regul Integr Comp Physiol* **268**, R752–R758.

Walker SC & Winn P (2007). An assessment of the contributions of the pedunculopontine tegmental and cuneiform nuclei to anxiety and neophobia. *Neuroscience* **150**, 273–290.

Watkins LL, Grossman P, Krishnan R & Sherwood A (1998). Anxiety and vagal control of heart rate. *Psychosom Med* **60**, 498–502.

Zemlan FP & Behbehani MM (1988). Nucleus cuneiformis and pain modulation: anatomy and behavioral pharmacology. *Brain Res* **453**, 89–102.

Zhang SH, Bandler R & Carrive P (1990). Flight and immobility evoked by excitatory amino acid microinjection within distinct parts of the subtentorial midbrain periaqueductal gray of the cat. *Brain Res* **520**, 73–82.

Author contributions

The experiments described in this paper were performed in UPMC/INSERM Faculty of medicine, Paris, France. Conception and design of experiments: C.S-C; collection, analysis and interpretation of data: F.N., C.S.-C., J.F.B. and F.C.; drafting the article and revisions: C.S.-C., A.J.M.V., J.J.B., M.H. and J.F.B.

Acknowledgements

This research was supported by grants from INSERM and Université Pierre et Marie Curie. We are especially grateful to Prof. David Julius (USCF, USA) for a generous gift of 5-HT_3 knock-out mice from which our breeding colony was derived. The authors would like to thank Dr Jean-Jacques Benoliel for his judicious remarks on the manuscript.